First-principles study on superconductivity in alkali-doped fullerides

Ryotaro ARITA
RIKEN Center for Emergent Matter Science
Wako, Hirosawa, Saitama 351-0198
Isobe Degenerate π-Integration Project, JST, ERATO
Aoba-ku, Sendai 980-8577

Abstract

Superconductivity in alkali-doped fullerides (A_3C_{60}) is of great interest in particular due to its high transition temperature (T_c) that is the highest among molecular solids. In the phase diagram, the superconducting phase resides next to a Mott-insulating phase. While this situation is similar to that of cuprates, superconductivity in A_3C_{60} is more non-trivial and interesting, since the gap function has an on-site s-wave symmetry for which one usually expects that local electron correlations causing the Mott-Hubbard transition severely suppress its T_c. To clarify the pairing mechanism of A_3C_{60}, we recently performed first-principles studies based on superconducting density functional theory (SCDFT) and multi-scale *ab initio* scheme for correlated electron systems (MACE). Our results establish that the multi-orbital electronic correlations and phonons cooperate to reach high T_c s-wave superconductivity in A_3C_{60}.

1 Introduction

Superconductivity in alkali-doped fullerides (A_3C_{60}) was discovered in 1991[1]. At that time, the transition temperature (T_c ∼40K) was the second highest which was only surpassed by the cuprates. Since then, the pairing mechanism of the high T_c superconductivity has been attracting broad interest. In Ref.[2], Yildirim *et al.* made a famous plot for T_c as a function of the lattice constant a of the system, which clearly shows that T_c and a (or the volume per C_{60}^{-3}) has a positive correlation. This result can be understood in terms of the standard BCS theory, in which T_c is given by the following equation:

$$T_c = \omega_{\rm ph} \exp(\frac{-1}{N_F V_{\rm eff}}),$$

where ω_{ph}, N_F and $V_{\rm eff}$ represent the averaged phonon frequency, the density of states at the Fermi level and the attractive pairing interaction, respectively. Since the band width becomes narrower for larger a, we expect larger N_F and higher T_c. Namely, a and T_c should have a positive correlation.

Recently, a new experimental method to synthesize highly crystalline Cs-doped fullerides has been established, and the phase diagram is extended to the region for larger a[3, 4, 5]. There, it has been shown that the superconducting phase has a dome-like shape, and resides next to a Mott insulating phase.

Motivated by these experimental observations, we recently performed first-principles calculations to investigate the pairing mechanism of A_3C_{60}. One is a study based on the density functional theory for superconductors (SCDFT)[6, 7, 8, 9], and the other is based on the multi-scale *ab initio* scheme for correlated electron systems (MACE)[10].

In the former, we calculated T_cs for K_3C_{60}, Rb_3C_{60} and Cs_3C_{60} to examine the validity of the Migdal-Eliashberg theory[11]. We found that the theoretical values of T_c are systematically lower than half of the experimental values. This result strongly suggests that we have to go beyond the Migdal-Eliashberg theory to

understand the high T_c superconductivity in A_3C_{60}.

In the latter, we formulated a new scheme to derive electron-phonon coupled models from first principles[12], and applied it to A_3C_{60}. After we determined all the relevant parameters in the effective Hamiltonian, we solve it by means of the extended dynamical mean field theory (EDMFT)[13]. The experimental values of T_c and the phase boundary of the Mott-Hubbard transition was successfully reproduced at a quantitative level[14].

2 Validity of the Migdal Eliashberg theory

Let us first examine whether the high T_c superconductivity in A_3C_{60} can be understood in terms of the conventional Migdal Eliashberg theory. To this end, we performed a calculation based on SCDFT. SCDFT is an extension of DFT for normal states to superconducting states. In the standard DFT, we start with the Hohenberg-Kohn theorem[15] which guarantees the one-to-one correspondence between the charge density of the ground state (ρ) and the external potential v. In SCDFT, we introduce the anomalous density ρ_s on top of the normal density ρ, and the Hohenberg-Kohn theorem is extended to a one-to-one correspondence between two kinds of potential (v, Δ) and two kinds of density (ρ, ρ_s). Then the Kohn-Sham equation[16] is extended to the Kohn-Sham Bogoliubov-de Gennes equation from which we can derived the linearized gap equation,

$$\Delta = \frac{-1}{2} \sum_j \mathcal{K}_{ij} \frac{\tanh[\beta\xi_j/2]}{\xi_j} \Delta_j, \qquad (1)$$

where ξ and β are the Kohn-Sham energy and inverse temperature, respectively. The kernel of the gap equation, $\mathcal{K}_{ij}$, is obtained by taking the second functional derivative of the exchange correlation functional[6, 7, 8, 9].

Here, it should be noted that $\mathcal{K}$ is a universal functional. Therefore, one can calculate T_c from first principles for any materials once he obtains the exact form of $\mathcal{K}$. In fact, recently, $\mathcal{K}$ for conventional phonon-mediated superconductors has been proposed[8, 9], and has been successfully employed in the calculations for a variety of systems. In Fig.1, we show a benchmark result for Al and Nb. Here, we plot the gap function Δ at the Fermi level as a function of temperature T. Δ vanishes at $T = T_c$, and we see that the agreement between the theoretical and experimental T_cs is remarkably good. Thus the kernel $\mathcal{K}_{ij}$ proposed in Ref.[8, 9] successfully takes account of the physics of the Migdal-Eliashberg theory, i.e., the retardation effect and the mass enhancement effect due to the electron-phonon coupling.

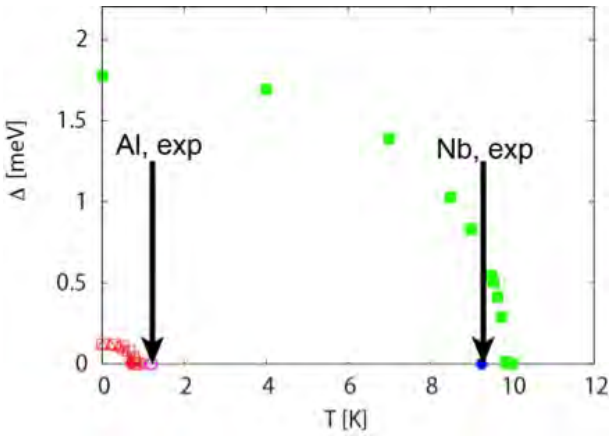

Figure 1: Temperature dependence of the gap function in SCDFT calculated for Al and Nb. Experimental T_cs are indicated by arrows.

We then studied whether SCDFT with the same kernel $\mathcal{K}_{ij}$ reproduces the experimental T_c for A_3C_{60}. In Fig.2, we see that the theoretical T_cs are systematically lower than the experimental values. This trend is very different from the situation in many conventional superconductors, which raises a question on the validity of the Migdal-Eliashberg theory for doped fullerides.

3 Analysis based on Multi-scale *ab initio* scheme

3.1 Low-energy Hamiltonian

Let us here move on to another approach based on MACE[10]. In this approach, we first derive

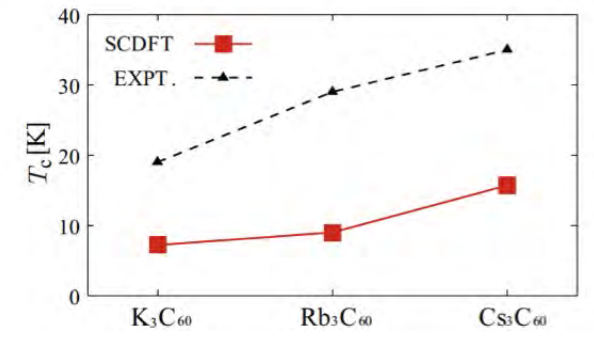

Figure 2: Superconducting transition temperature (T_c) calculated for K_3C_{60}, Cs_3C_{60} and Cs_3C_{60}.

an effective low energy model from first principles and then solve it by modern many-body theory.

In Fig.3, we show the band structure of K_3C_{60} obtained by the standard density functional theory[17]. There are three t_{1u} bands around the Fermi level, which are well isolated from other high-energy bands. In the present study, we are going to construct an effective low energy model for the t_{1u} model.

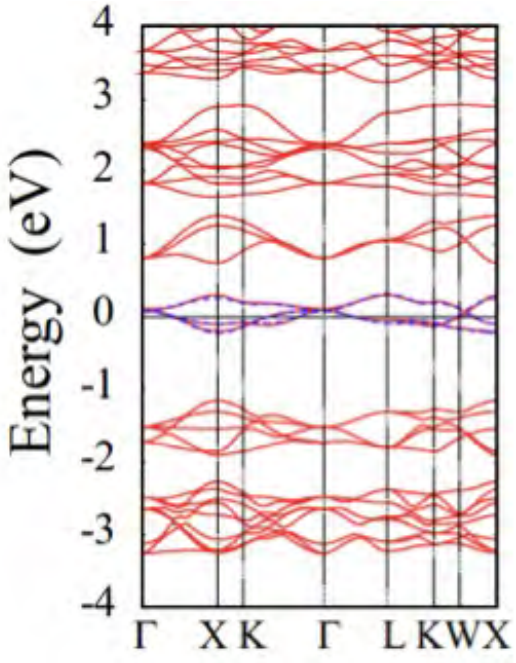

Figure 3: Band structure of K_3C_{60}. Wannier-interpolated t_{1u} bands are indicated by blue dotted lines.

The Hamiltonian is given by

$$\begin{aligned}\mathcal{H} &= \sum_{\mathbf{k}}\sum_{ij}[H_0(\mathbf{k})]_{ij}c^\dagger_{i\sigma}(\mathbf{k})c_{j\sigma}(\mathbf{k}+\mathbf{q}) \\ &+\sum_{\mathbf{q}}\sum_{\mathbf{k},\mathbf{k}'}\sum_{i,i',j,j'}U_{i,j,i',j'}(\mathbf{q}) \\ &c^\dagger_{i\sigma}(\mathbf{k}+\mathbf{q})c^\dagger_{i'\sigma'}(\mathbf{k}')c_{j'\sigma'}(\mathbf{k}'+\mathbf{q})c_{j\sigma}(\mathbf{k}) \\ &+\sum_{\mathbf{q}\nu}\sum_{\mathbf{k}}\sum_{i,j}\sum_{\sigma}g_{ij\nu}(\mathbf{k},\mathbf{q}) \\ &c^\dagger_{i\sigma}(\mathbf{k}+\mathbf{q})c_{j\sigma}(\mathbf{k})(b_\nu(\mathbf{q})+b^\dagger_\nu(-\mathbf{q})) \\ &+\sum_{\mathbf{q}\nu}\omega_\nu(\mathbf{q})b^\dagger_\nu(\mathbf{q})b_\nu(\mathbf{q}),\end{aligned}$$

where $c^\dagger_{i\sigma}(\mathbf{k})$ ($c_{i\sigma}(\mathbf{k})$) is a creation (annihilation) operator for the i-th orbital electron having spin σ and momentum $\mathbf{k}$. $b^\dagger_\nu(\mathbf{q})$ ($b_\nu(\mathbf{q})$) is a creation (annihilation) operator for a phonon having momentum $\mathbf{q}$ in the ν-th branch.

The first term in the Hamiltonian (2) is the one-body term of electrons. To derive this term, following the procedure formulated in Ref.[18], we constructed three maximally localized Wannier functions from the t_{1u} band (one of which is shown in in Fig.4). As we can see in Fig.3, the Wannier interpolated band reproduces the original band dispersion in the DFT calculation.

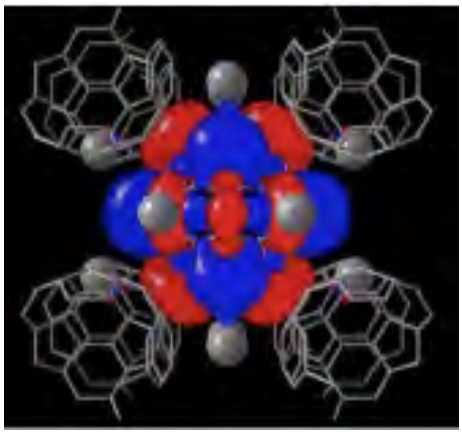

Figure 4: One of the three maximally localized Wannier functions constructed from the t_{1u} bands. Sign of the wave function is indicated in blue and red.

3.2 Electron-correlation terms

The second term in eq.(2) represents electron correlations, which consists of density-density

interactions such as the Hubbard U and exchange interactions like the Hund's coupling J. When we evaluate these interaction parameters, we have to carefully treat the screening effect. Since screening by low-energy electrons are considered when we solve the effective model, we should exclude its contributions when we derive the model. To this end, we employed the constrained random phase approximation (cRPA)[19].

In RPA, the screened Coulomb interaction W is given by

$$W = (1 - v\chi)^{-1} v,$$

where v is the bare Coulomb interaction, and χ is the polarizability,

$$\chi = \sum_{i}^{occupied} \sum_{j}^{unoccupied} \frac{\psi_i(\mathbf{r})\psi_j^*(\mathbf{r})\psi_i^*(\mathbf{r}')\psi_j(\mathbf{r}')}{\omega - \epsilon_j + \epsilon_i}.$$

Here, ψ_i is the i-th Bloch wave function having an eigenenergy of ϵ_i. Let us call ψ_i "occupied state" ("virtual state") when ϵ_i is lower (higher) than those of the t_{1u} bands. In χ, there are four types of processes: Transitions from occupied states to the t_{1u} states, those from the t_{1u} states to virtual states, those from occupied states to virtual states, and transitions between the t_{1u} states. In cRPA, we calculate "partially" screened Coulomb interaction without the contribution of the last transition processes.

In Fig.5, we show the correlation strength $(\bar{U} - \bar{V})/W$ for fcc A_3C_{60} (A=K, Rb and Cs), where $\bar{U}$ is the averaged onsite Hubbard interaction, $\bar{V}$ is the offsite Coulomb interaction between neighboring sites, and W is the band width of the t_{1u} band, respectively[20]. For A=Cs, we performed calculations for three volumes, i.e., where T_c takes its maximum ($V_{\rm SC}^{\rm opt.P}$), where the metal-insulator transition occurs ($V_{\rm MIT}$) and where the system is an antiferromagnetic insulator ($V_{\rm AFI}$). We see that the electron correlation is stronger than the band width in all the five cases. Here, it is interesting to note that Cs_3C_{60} having higher T_c has stronger electronic correlations than K_3C_{60}. This trend cannot be understood in terms of the standard BCS theory, where the Coulomb interaction always suppresses superconductivity.

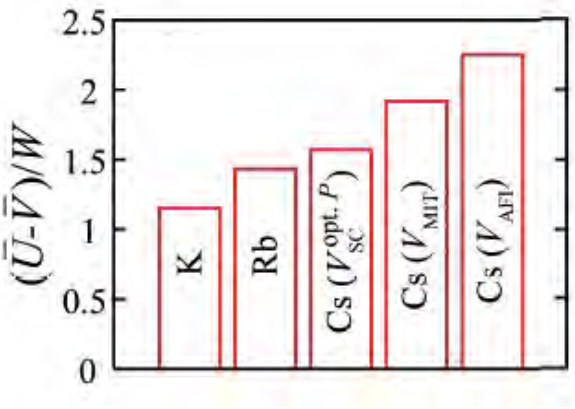

Figure 5: Correlation strength $(\bar{U} - \bar{V})/W$ calculated by cRPA for A_3C_{60} (A=Cs, K and Rb).

In Fig.6, we plot the values of the Hund's coupling J for A_3C_{60}. We see that the size of J is as large as 0.03eV. Since U is ∼1eV, the ratio J/U is less than 5 %, which is much smaller than a typical value for transition metal compounds[21], 10 ∼ 20%. This is because the spreads of Wannier functions are huge for molecular systems. In fact, as we will see below, the energy scale of the antiferromagnetic exchange coupling $J_{\rm ph}$ due to the dynamical Jahn-Teller effect is as large as that of J. The competition between $J_{\rm ph}$ and J is of great interest, since unconventional superconductivity can emerge when the former dominates over the latter[22, 23].

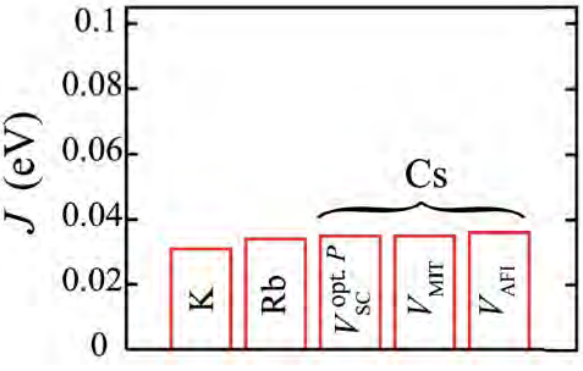

Figure 6: Hund's coupling J calculated by cRPA for A_3C_{60} (A=Cs, K and Rb).

3.3 Phonon terms

Let us now look into the detail of the competition between J and $J_{\rm ph}$. To calculate the value of $J_{\rm ph}$ from first principles, we evaluated the electron-phonon coupling $g_{ij\nu}(\mathbf{k},\mathbf{q})$ and the phonon ferquency $\omega_\nu(\mathbf{q})$ in the third and fourth term in the Hamiltonian (2). Here, as in the case of cRPA, we should take account only of screening by high energy electrons. To this end, we recently formulated a new scheme, which we call constrained density functional perturbation theory (cDFPT)[12].

In the standard DFPT, the electron-phonon coupling is estimated by calculating the matrix element of

$$\langle\psi_{i\mathbf{k}+\mathbf{q}}|\frac{\partial v}{\partial u}|\psi_{j\mathbf{k}}\rangle,$$

where v is the atomic potential and u is the displacement of nuclei. On the other hand, the phonon frequency is obtained by taking the second derivative of the total energy E with respect to u. Since all the physical quantities in DFT are represented in terms of the electron density ρ, if we know the response of ρ against u, we can evaluate $g_{ij\nu}(\mathbf{k},\mathbf{q})$ and $\omega_\nu(\mathbf{q})$ through the chain rule, $\partial/\partial u = \partial\rho/\partial u\partial/\partial\rho$. The response of the charge density $\Delta\rho$ can be calculated by the perturbation theory[24],

$$\begin{aligned}\Delta\rho &= 2\sum_i \psi_i^*\Delta\psi_i,\\ \psi_i &= \sum_{i\neq j}\psi_j\frac{\langle\psi_j|\Delta V|\psi_i\rangle}{\varepsilon_i-\varepsilon_j}.\end{aligned}$$

In cDFPT, we introduce a constraint in the sum over j, and exclude the contribution of the t_{1u} states. Then we obtain partially screened $g_{ij\nu}(\mathbf{k},\mathbf{q})$ and $\omega_\nu(\mathbf{q})$.

The phonon-mediated exchange coupling $J_{\rm ph}$ is given by

$$J_{\rm ph} = -\sum_{\mathbf{q}\nu} g_{ij\nu}(\mathbf{k},\mathbf{q})\frac{2\omega_\nu(\mathbf{q})}{\Omega_n^2+\omega_\nu^2(\mathbf{q})}g_{ji\nu}(\mathbf{k},\mathbf{q}),$$

where Ω_n is the bosonic Matsubara frequency (see the Feynman diagram in Fig. 7). We estimated $J_{\rm ph}$ for A_3C_{60} (A=K, Rb, and Cs) and found that $J_{\rm ph}$ is negative and favors low-spin configurations. While the absolute value of J is 0.03$\sim$ 0.035 eV and does not show significant frequency dependence, that of $J_{\rm ph}$ is $\sim$ 0.05 eV for small Ω_n and decays quickly within the energy scale of the Debye frequency. Thus for low-energy electrons, $J_{\rm ph}$ dominates over J.

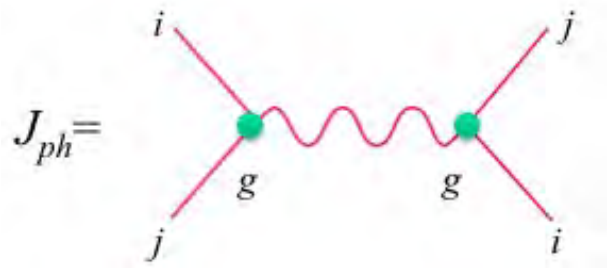

Figure 7: Diagram for the phonon-mediated exchange coupling $J_{\rm ph}$. The wavy line denotes the Green's function of phonons.

In Ref.[22, 23], Capone *et al.* proposed an interesting unconventional pairing mechanism for strongly correlated multi-orbital systems with inverted Hund's rule coupling. When the electron correlations become stronger, the effective mass of the quasiparticle becomes heavier and the energy scale of the kinetic energy becomes smaller as $W \to ZW$, where Z is the quasiparticle weight. While the heavy quasiparticle experiences reduced repulsion ZU in the charge channel, the interaction in the spin channel $J_{\rm eff} = J + J_{\rm ph}$ is not renormalized. Namely, the spin degrees of freedom is still active even when the charge fluctuations are frozen. Thus, when Z is extremely small in the vicinity of the Mott insulating phase, the quasiparticles feel attractive interactions which induce unconventional s-wave superconductivity. Although the symmetry of the gap function is on-site s-wave, this superconducting phase is sometimes separated from the conventional BCS superconducting phase in the phase diagram.

3.4 Extended dynamical mean field theory

To investigate the possibility of high T_c s-wave superconductivity in the vicinity of the Mott insulating phase, we then solve the effective low-energy model derived in the previous subsection by means of EDMFT[13]. In DMFT, we map the original lattice many-body prob-

lem onto a single-site impurity problem and solve it self-consistently. DMFT has been applied to various problems in strongly correlated electron systems, and has succeeded in describing physics of local electron correlations[25].

In EDMFT, we can take account of the effect of off-site long-range Coulomb interaction. There, the momentum dependence of the Coulomb interaction in the original lattice model is represented by the frequency dependent Hubbard $U_V(\omega)$ in the impurity model. The effect of electron-phonon coupling can also be represented by the frequency dependent Hubbard $U_{\rm ph}(\omega)$[26, 27].

In Fig.8, we show the Matsubara-frequency dependence of the effective intra- and inter-orbital interactions ($U_{\rm eff}(i\Omega_n)$ and $U'_{\rm eff}(i\Omega_n)$, respectively) in the impurity model. Due to screening by the off-site Coulomb interaction, the Hubbard U and U' in the original lattice model is reduced to be $U + U_V = U - V$ and $U' + U'_V = U' - V'$ at $\Omega_n \to 0$. As for the relation between U and U', $U = U' + 2J$ holds in the original lattice model. Since the Hund's coupling J is positive and favors high-spin states, $U > U'$. In Fig.8, we can see that the same inequality is also satisfied for $U + U_V$ and $U' + U'_V$.

However, the situation changes if we consider the contribution of $U_{\rm ph}$ and $U'_{\rm ph}$. As we have seen in the previous subsection, $J_{\rm ph}$ dominates over J, so that $U + U_V + U_{\rm ph} < U' + U'_V + U'_{\rm ph}$ for small Ω_n. Therefore, in the impurity model, electrons tend to occupy the same orbital, rather than different orbitals (the so-called (2,1,0)-configurations shown in Fig.9). On top of that, there are pair-hopping processes between various (2,1,0)-configurations governed by the negative $J_{\rm eff} = J + J_{\rm ph}$,

Let us now turn to the phase diagram. We solved the effective impurity model by means of continuous time quantum Monte Carlo method based on the strong coupling expansion[28], considering explicitly the anomalous Green's function. We calculated T_c by looking at the temperature dependence of the anomalous self energy. We also determined the phase boundary between the metallic (superconducting) state and the Mott insulating phase ($T_c^{\rm MIT}$). We calculate T_c and $T_c^{\rm MIT}$ as a

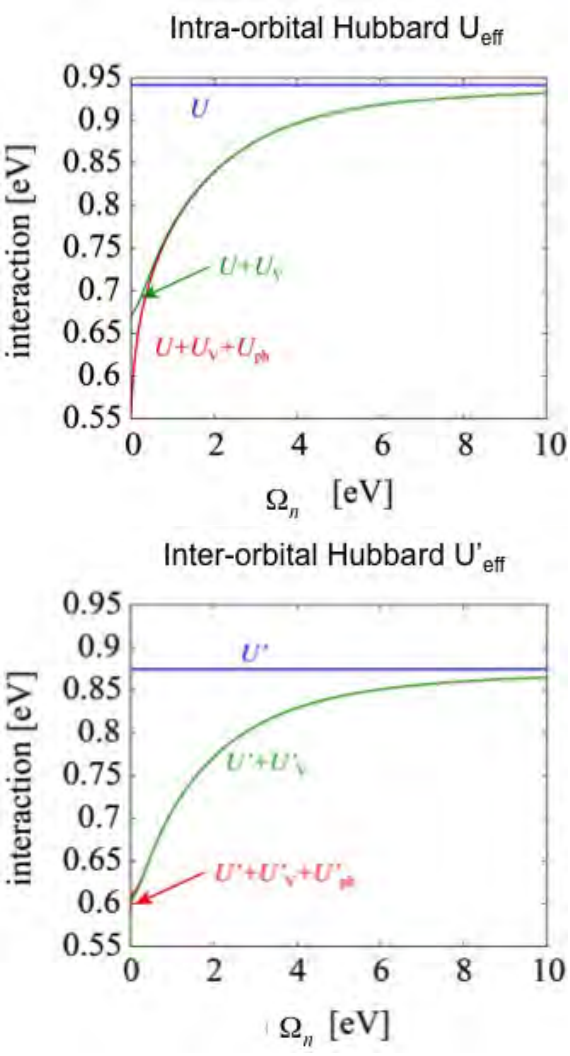

Figure 8: Matsubara frequency dependence of the intra-(inter-)orbital Hubbard $U_{\rm eff}(U'_{\rm eff})$ parameters in the effective impurity model in EDMFT.

function of the volume of the unit cell ($V_{C_{60}^{-3}}$). As we can see in Fig.10, $T_c = 20 \sim 30$K for $V_{C_{60}^{-3}} = 720 \sim 780$Å^3, which is in quantitatively good agreement with the experimental phase diagram[29]. As for the Mott-Hubbard transition, $T_c^{\rm MIT}$ has a negative slope and becomes zero at $V_{C_{60}^{-3}} \sim 780$Å^3, which also agrees well with the experiment[29].

To pin down the origin of the high T_c superconductivity, we have performed some additional calculations. First, we switched off the pair hopping term, keeping the values of the other interaction terms. We then found

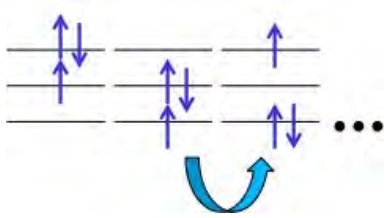

Figure 9: Schematic picture for the (2,1,0) configuration.

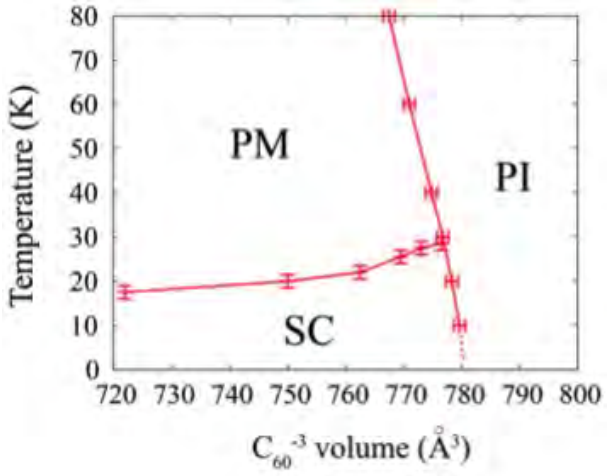

Figure 10: Phase diagram obtained by EDMFT calculation.

that there is no superconducting solution. On the other hand, if we switched off the spin flip term, the superconducting solution survives and is even enhanced. These results suggest that the pair hopping (spin flip) term is crucial (irrelevant) for superconductivity. Here, it should be noted that, although the energy scale of the pair hopping term is very small ($J_{\rm eff} = J + J_{\rm ph}$), the effective band width is also small due to the strong electron correlations (U and U').

We have also performed a calculation with increasing the attractive phonon-mediated inter-orbital interaction and set $U'_{\rm ph} = U_{\rm ph}$. Here, while $U'_{\rm eff}$ is less repulsive, the inequality $U_{\rm eff} > U'_{\rm eff}$ holds for all Matsubara frequencies. In this case, there is no superconducting solution. Therefore, the condition $U_{\rm eff} < U'_{\rm eff}$ at small frequencies is also important for the superconductivity in this system.

4 Summary

In this article, we have reviewed our recent first-principles studies on superconductivity in alkali-doped fullerides, A_3C_{60}. To study the validity of the standard Migdal-Eliashberg theory, We performed calculations based on SCDFT and compared the theoretical and experimental values of T_c. We found that SCDFT systematically underestimate T_c, which suggests that the high T_c superconductivity in doped fullerides can not be understood in terms of the the standard conventional mechanism.

In the approach based on MACE, we formulated a new scheme, cDFPT, to derive electron-phonon coupled effective models from first principles. We then solve the effective model within the framework of EDMFT, and succeeded in reproducing the experimental phase diagram quantitatively, including the superconducting phase and Mott insulating phase. We clarified that the negative Hund's coupling and the condition $U_{\rm eff} < U'_{\rm eff}$ are crucial for the high T_c superconductivity in A_3C_{60}. These results establish that doped fullerides are unique multi-orbital systems where electronic correlations and phonons cooperate to realize high T_c s-wave superconductivity.

Acknowledgement

This work was done in collaboration with Y. Nomura, R. Akashi, S. Sakai, K. Nakamura and M. Capone.

References

[1] O. Gunnarsson: Rev. Mod. Phys., **69** 575 (1997).

[2] T., Yildirim *et al.*: Solid State Commun. **93**, 269 (1995).

[3] A. Y. Ganin *et al.*: Nat. Mater. **7**, 367 (2008).

[4] Y. Takabayashi *et al.*: Science **323**, 1585 (2009)

[5] A. Y. Ganin *et al.*: Nature **466**, 221 (2010).

[6] L. N. Oliveira *et al.*: Phys. Rev. Lett. **60**, 2430 (1988).

[7] T. Kreiblich and E.K.U. Gross: Phys. Rev. Lett. **86**, 2984 (2001).

[8] M. Lüders *et al.*, Phys. Rev. B **72**, 024545 (2005).

[9] M. Marques *et al.*, Phys. Rev. B **72**, 024546 (2005).

[10] M. Imada and T. Miyake: J. Phys. Soc. Jpn, **79** 112001 (2010).

[11] R. Akashi and R. Arita, Phys. Rev. B **88** 054510 (2013).

[12] Y. Nomura, K. Nakamura, and R. Arita: Phys. Rev. Lett. **112** 027002 (2014).

[13] G. Kotliar *et al.*: Rev. Mod. Phys. **78** 865 (2006)

[14] Y. Nomura, S. Sakai, M. Capone, and R. Arita: submitted.

[15] P. Hohenberg and W. Kohn: Phys. Rev. **136**, B864-B871 (1964).

[16] W. Kohn and L.J. Sham: Phys. Rev. **140**, A1133-1138 (1965).

[17] In the present study, we used the package of QUANTUM ESPRESSO, P. Giannozzi *et al.*,: J.Phys.:Condens.Matter, **21**, 395502 (2009)

[18] N. Marzari and D. Vanderbilt: Phys. Rev. B **56**, 12847 (1997).

[19] F. Aryasetiawan *et al.*: Phys. Rev. B **70** 195104 (2004).

[20] Y. Nomura, K. Nakamura, and R. Arita: Phys. Rev. B **85** 155452 (2012).

[21] T. Miyake, K. Nakamura, R. Arita, and M. Imada: J. Phys. Soc. Jpn. **79** 044705 (2010)

[22] M. Capone *et al.*: Science **296**, 2364 (2002).

[23] M. Capone *et al.*: Rev. Mod. Phys. **81**, 943 (2009).

[24] S. Baroni *et al.*, Rev. Mod. Phys. **73**, 515 (2001).

[25] A. Georges *et al.*: Rev. Mod. Phys. **68**, 13 (1996)

[26] I.G. Lang and Y. A. Firsov: Zh. Eksp. Teor. Fiz. 43, 1843 (1962).

[27] P. Werner and A. J. Millis, Phys. Rev. Lett. **104**, 146401 (2010).

[28] E. Gull *et al.*: Rev. Mod. Phys. **83**, 349 (2011).

[29] R. H. Zadik *et al.*, to appear in Science Advances (2015).